Vibrational and Orientational Dynamics of Water in Aqueous Hydroxide Solutions

Johannes Hunger, Liyuan Liu, Klaas-Jan Tielrooij, Mischa Bonn, and Huib Bakker

FOM Institute AMOLF, Science Park 104,

1098 XG Amsterdam, The Netherlands, h.bakker@amolf.nl

(Dated: November 5, 2012)

Abstract

We report the vibrational and orientational dynamics of water molecules in isotopically diluted NaOH and NaOD solutions using polarization-resolved femtosecond vibrational spectroscopy and terahertz time-domain dielectric relaxation measurements. We observe a speed-up of the vibrational relaxation of the O–D stretching vibration of HDO molecules outside the first hydration shell of OH^- from 1.7±0.2 ps for neat water to 1.0±0.2 ps for a solution of 5 M NaOH in HDO:H_2O. For the O–H vibration of HDO molecules outside the first hydration shell of OD^-, we observe a similar speed-up from 750±50 fs to 600±50 fs for a solution of 6 M NaOD in HDO:D_2O. The acceleration of the decay is assigned to fluctuations in the energy levels of the HDO molecules due to charge transfer events and charge fluctuations. The reorientation dynamics of water molecules outside the first hydration shell are observed to show the same time constant of 2.5±0.2 ps as in bulk liquid water, indicating that there is no long range effect of the hydroxide ion on the hydrogen-bond structure of liquid water. The THz dielectric relaxation experiments show that the transfer of the hydroxide ion through liquid water involves the simultaneous motion of ∼7 surrounding water molecules, considerably less than previously reported for the proton.

I. INTRODUCTION

The hydroxide ion (OH^-) and the proton (H^+) both have very high mobilities in aqueous solution compared to other ions.[1] These high mobilities result from the special transport mechanism of H^+ and OH^- in water. In this mechanism charge transport does not require actual mass transport, but only breaking and reformation of hydrogen bonds. This concept was introduced by Grotthuss as early as 1806.[2]

Despite the fact that aqueous OH^- and H^+ solutions are often referred to as mirror systems, the mobilities of OH^- and H^+ in water differ by a factor of ~ 2.[1] This difference has stimulated a large number of experimental[3–8] and theoretical[9–11] studies attempting to elucidate the role of the hydration structures of H^+ and OH^- on the transport properties. From these studies it became clear that the properties of aqueous solutions of acids and bases cannot be simply modeled as an excess proton and a proton hole in the three-dimensional hydrogen-bonded network of water. In fact it has been found that the hydration structure of H^+ and OH^- are remarkably different (see e.g. ref. 11 for an overview), and are by no means each others mirror image.

Ultrafast infrared spectroscopies[3,4,12] have provided valuable insights into the structural and dynamical aspects of aqueous solutions. For aqueous solutions of OH^-, a very fast vibrational relaxation component has been observed with a time constant of 120 - 160 fs.[3,4] This fast component has been assigned to the relaxation of OH groups of water next to a $OH^- \cdots OH_2$ complex showing charge transfer (spectator mode),[4] and to the Zundel-like transition state of the $OH^- \cdots OH_2$ system itself.[3] In a recent femtosecond two-dimensional spectroscopic study, the proton transfer between the hydroxide ion and the water has been measured, leading to the effective motion of the hydroxide ion. This transfer was found to take place on a relatively long time scale with a lower boundary of 3 picoseconds.[13]

For the proton in water, it has been demonstrated both theoretically[14] and experimentally[15] that water molecules well beyond the first solvation shell are involved in proton transport. Up to 20 water molecules were shown to be affected by the presence of the proton.[15] Despite its significance for the ion transport, up to now little attention has been paid to the influence of alkaline environment on the dynamical properties of the water phase beyond the water molecules that directly interact with the OH^- ion. There have been a few scattering experiments[5,8,16] that suggest that the overall hydrogen-bonded structure

of hydroxide solutions is more compact than in bulk liquid water.

Here we report on a detailed polarization-resolved femtosecond vibrational spectroscopic study of the influence of NaOH on the vibrational energy relaxation and molecular reorientation of water molecules that are not directly bound to the hydroxide ion. We performed experiments on the O–D stretching vibration of HDO molecules in a solution of 4 % D_2O in H_2O and on the O–H vibration of HDO molecules in a solution of 4 % H_2O in D_2O as a function of NaOH and NaOD concentration, respectively, at ambient conditions. We performed complementary studies of the water reorientation using transient Terahertz dielectric relaxation spectroscopy.[15,17] In order to investigate the influence of the cation on these experiments, aqueous solutions of both NaOH and KOH were investigated.

II. EXPERIMENTAL METHODS

A. Femtosecond Infrared Measurements

Femtosecond infrared pump and probe pulses were generated via a sequence of nonlinear optical conversion processes that are pumped by a commercial Ti:sapphire regenerative amplifier system. This system delivers pulses at 800 nm with a duration of 100 fs at a repetition rate of 1 kHz (1 mJ per pulse). Approximately 0.7 mJ of pulse energy is used to pump an optical parametric amplifier (OPA) based on a β-barium borate (BBO) crystal. In this process idler pulses at $\sim 2\,\mu$m are generated that are subsequently frequency-doubled in a second BBO crystal, yielding pulses of $\sim 1\,\mu$m. For the experiments on O–H oscillators, 1.1 μm pulses are generated and used as seed pulse in a parametric amplification process in a potassium titanium oxide phosphate crystal (KTP). This process is pumped with the remaining 0.3 mJ of the 800 nm pulses, and yields mid-infrared pulses with a duration of ~ 200 fs, a center frequency of 3400 cm^{-1} and an energy of 2.5 μJ. To excite O–D oscillators, pulses centered at 2500 cm^{-1} were generated in a similar manner by mixing doubled-idler pulses at 1 μm with 800 nm pulses in a potassium niobate crystal. This latter process yields pulses with a duration of 150 fs and an energy of $\sim 4\,\mu$J.

The mid-infrared pulses are split by a CaF_2 wedged window. The reflections at the front and the back sides of the wedged window are used as probe and reference pulses, respectively. The transmitted pulse is used as the pump. With a $\lambda/2$ plate the polarization of the pump

pulse is set to an orientation of 45 ° with respect to the probe and the reference polarization. The time delay of the probe pulses with respect to the pump is varied via a variable path-length delay line. The three pulses are focused into the sample that is held between two CaF_2 windows. The foci of the probe and pump overlap. After passing a polarizer that allows us to select the parallel or perpendicular (with respect to the pump) polarization components, the probe and reference beams are sent into a spectrometer dispersing the beams on a liquid-nitrogen-cooled mercury-cadmium telluride detector. The probe pulse is used to measure the (pump-induced) transient absorption in the sample parallel ($\Delta\alpha_{\parallel}(\omega, t)$) and perpendicular ($\Delta\alpha_{\perp}(\omega, t)$) to the pump polarization as a function of delay time, t, and wavenumber, ω. The reference pulse is used for a spectrally resolved correction of the pulse to pulse energy fluctuations.[18]

From the measured absorption changes $\Delta\alpha_{\parallel}(\omega, t)$ and $\Delta\alpha_{\perp}(\omega, t)$ the isotropic signal can be constructed:

$$\Delta\alpha_{\mathrm{iso}}(\omega, t) = \frac{\Delta\alpha_{\parallel}(\omega, t) + 2\Delta\alpha_{\perp}(\omega, t)}{3} \tag{1}$$

The isotropic signal is independent of reorientation processes. Complementary to the isotropic signal the anisotropy parameter $R(t)$ can be constructed:

$$\Delta R(\omega, t) = \frac{\Delta\alpha_{\parallel}(\omega, t) - \Delta\alpha_{\perp}(\omega, t)}{3\Delta\alpha_{\mathrm{iso}}(\omega, t)}. \tag{2}$$

The parameter $R(t)$ is independent of vibrational relaxation and only reflects the reorientation dynamics of the excited molecules.

B. Terahertz Measurements

We used a terahertz time-domain spectrometer (THz-TDS) to measure complex permittivity spectra, $\hat{\eta}(\nu)$, at frequencies $0.4 \leq \nu/\mathrm{THz} \leq 1.6$ which may contain contributions from conductivity and dipolar relaxations.[15] Terahertz pulses are generated in a ZnTe (110) nonlinear crystal from 800 nm pulses with a duration of ~ 150 fs from a Ti:Sapphire laser.[19] The generated THz pulses have a duration of ~ 1 ps. The time-dependent electric field of the THz pulse is measured via its electro-optic effect on a variably delayed 800 nm laser pulse in a second ZnTe crystal. A frequency domain analysis of the THz pulse transmitted through an empty cell (Infrasil quartz, path length $103 \pm 0.5\,\mu$m) and the THz pulse

transmitted through a filled sample cell, yields the frequency dependent complex index of refraction ($\hat{n} = n - \mathrm{i}k$). In analysing the data, all (multiple) reflection and transmission coefficients for all transitions (air-quartz-sample-quartz-air) were taken into account.[20] To minimize the effect of fluctuations in the THz intensity, a mechanical device was used to position the sample and a pure water reference alternatingly in the focus of the THz beam. The neat water data were used to calibrate the spectra of the samples.

For pure water the dielectric spectrum is dominated by a strong mode at $\sim 20\,\mathrm{GHz}$ that can be described well with a Debye equation (i.e. a single exponential decay of the orientational polarization of the sample). The dominant orientational mode has a broad frequency response that extends to THz frequencies and thus the amplitude of this mode can be detected by transient THz spectroscopy.[15,21] This mode represents the collective reorientation of the hydrogen-bonded network of water and has a characteristic relaxation time of $\tau \approx 8.3\,\mathrm{ps}$.[22] The dielectric relaxation time is proportional to the first-order correlation time, in contrast to the fs-infrared experiment, that measures the second order orientational correlation time. As a result, the time constants measured with the two techniques differ by a factor of ~ 3.[23,24] This ratio is not exactly 3, because dielectric relaxation probes the macroscopic polarization whereas the fs-infrared experiment probes the local dynamics. This effect increases the ratio of the first and second order rotational correlation time constants. In addition, for water the reorientation takes place via large angle jumps. This effect makes the ratio somewhat smaller.[25] The net result of the two effects is that the ratio between the Debye time and the time constant measured in fs-infrared spectroscopy is $\sim$3.4.

The dielectric response of water not only contains the strong mode at 20 GHz, but also a much weaker mode at $\sim 0.5\,\mathrm{THz}$. This mode has been attributed to under-coordinated water[26] or to translational components in the water relaxation mechanism.[27] At even higher frequencies vibrational contributions like e.g. hydrogen-bond bending modes or librations are observed,[22] but these modes are above the frequency range of the present study.

For electrolyte solutions, both dipolar rotations and charge translations (conductivity) contribute to the dielectric response, $\hat{\eta}(\nu)$, of the sample. Assuming the conductivity, κ, to be real and independent of frequency (i.e. the dc conductivity), the frequency dependent complex permittivity, $\hat{\varepsilon}(\nu)$ $(= \hat{\eta}(\nu) - \mathrm{i}\kappa/(2\pi\nu\varepsilon_0))$ can be obtained, where ε_0 is the permittivity of free space. Note that by this approach $\hat{\varepsilon}(\nu)$ contains all frequency dependent contributions irrespective of their rotational or translational character.[28]

C. Samples

For the THz measurements aqueous solutions of sodium hydroxide (NaOH) and potassium hydroxide (KOH) were prepared by adding the appropriate amounts of water (HPLC grade, Sigma-Aldrich) to stock solutions of NaOH (analytical grade, 10 M, Sigma-Aldrich) and KOH ((28.5 ± 0.5) %, Fluka).

For the fs-IR experiments on the O–D vibration, isotopically diluted (4 % D_2O in H_2O) solutions of NaOH were prepared by adding a small amount of D_2O (99.9 %, Sigma-Aldrich) to a solution of NaOH in H_2O. The experiments on the O–H vibration were performed with the inverse system (4 % H_2O in D_2O), prepared from a 40 % solution of NaOD in D_2O (> 99 atom % D, Sigma-Aldrich) by adding the appropriate amounts of D_2O and H_2O. Linear infrared spectra, $\alpha(\omega)$, were measured using a double beam mid-infrared spectrometer (Perkin-Elmer 881). The samples were contained between two CaF_2 windows separated by a Teflon spacer. All solutions were prepared gravimetrically using an analytical balance. Densities, ρ, necessary for the calculation of molar concentrations, c, and conductivities,[29,30] κ required for analyzing THz measurements, were interpolated from literature values.[29–32]

III. RESULTS

A. Linear Infrared Spectra

The linear infrared spectra of aqueous hydroxide solutions show remarkable differences in comparison to the spectra of most other salt solutions. In addition to the absorption band of the O-H stretching vibration of HDO at $\sim 3400\,\mathrm{cm}^{-1}$, a continuous and featureless absorption at lower wavenumbers is observed.[3,12,33] As can be seen in Figure 1a, this absorption contribution increases with concentration of NaOH. This broad absorption is assigned to O–H vibrations of water molecules hydrating the hydroxide ion (O-H$\cdots$OH$^-$). At higher wavenumbers a stretching band of the hydroxide ion is observed in the form of a weak shoulder at $\sim 3600\,\mathrm{cm}^{-1}$ (Figure 1a). This band is mainly Raman active and only weakly present in the infrared spectra.[33,34]

For the O-D stretching vibration of HDO molecules at $\sim 2500\,\mathrm{cm}^{-1}$ similar features appear in concentrated solutions of NaOH in H_2O. However, due to the broad band absorption of O-H$\cdots$OH$^-$, the spectral response at $\sim 2500\,\mathrm{cm}^{-1}$ is not solely due to O-D vibrations. At

high concentrations of NaOH the contribution due to the O-H$\cdots$OH$^-$ background of H_2O molecules becomes increasingly pronounced and swamps the O-D stretching band (Figure 1b). The weak band at $\sim$2100 cm^{-1} is due to a combination vibration of H_2O.[35]

It is noteworthy that the contribution of the O-H$\cdots$OH$^-$ oscillators to the absorption is significantly weaker than that of water molecules hydrating the proton ($H_2O\cdots H^+$), as observed in acidic solutions.[12] The linear absorption spectrum of an acidic solution (in absence of deuterium) shows an approximately two times higher total absorbance at $\sim$ 2500 cm^{-1} than an aqueous solution of NaOH of the same concentration.

B. Femtosecond infrared spectroscopy

1. Isotropic Results

As shown in Figure 2a the isotropic transient spectra, after excitation at 2500 cm^{-1}, at O–D stretching frequencies at short delays are dominated by the characteristic spectral shape of a bleach ($\Delta\alpha_{\mathrm{iso}} < 0$, at $\sim$ 2500 cm^{-1} for the O–D stretch vibration) and an adjacent induced absorption (at $\omega <$ 2420 cm^{-1} for O–D) due to excited state absorption (1$\rightarrow$2 transition, Figure 2).[36] The excitation decays as t increases (Figure 2b). The bleach due to excited O–D oscillators dominating the isotropic signals at early delays broadens symmetrically as the concentration of NaOH increases (Figure 3a). A broadening of the O–D stretching band has already been observed with linear IR spectroscopy.[34] As will be discussed below, the broadening is less pronounced for the O–H stretching vibration (Figure 3b).

As can be seen from the linear spectra (Figure 1), excitation at 2500 cm^{-1} leads to excitation of not only the OD groups of water HDO, but with increasing OH$^-$ concentration also of O-H$\cdots$OH$^-$ groups that give rise to the continuous background. As has been shown previously, the excitation of these O–H oscillators is very short-lived with a vibrational lifetime $<$ 200 fs,[37] much shorter than the vibrational lifetime of $\sim$ 1.7 ps[38] of the O-D vibration of HOD. The observation of this short-lived component is in agreement with a very fast decaying component observed in an earlier time-resolved infrared study[4] and in two-dimensional infrared experiments.[3]

The pump pulse excitation eventually leads to heating of the sample by a few degrees. At long times ($t >$ 20 ps) this heating effect dominates the signal. The spectral signature of

the heating effect corresponds to a thermal difference spectrum (Figure 2a, dotted line).[36] For excitation of OD groups of HOD in H_2O solutions of OH^-, the broad O-H$\cdots$OH$^-$ background spectrum contributes to this thermal difference spectrum. An increase in temperature leads to a blueshift of the absorption band of the O-H$\cdots$OH$^-$ background (Figure 3a), thus making the thermal difference spectra more strongly bleached.

2. Data Analysis

To quantify the effect of the hydroxide ion on the vibrational relaxation we model the experimental isotropic transient spectra. In this study we only consider the data at $t > 500\,\mathrm{fs}$, for which the fast component of the OH$\cdots$OH$^-$ background has completely decayed. Hence, we only consider the vibrational relaxation of the O–D and O–H stretch vibrations of HDO molecules that are not directly hydrogen bonded to the hydroxide ion. The OD vibration of HDO decays with a significant longer time constant ($\sim 1.7\,\mathrm{ps}$ for pure HDO in H_2O) than the broadband background OH$\cdots$OH$^-$.[38] It was found in previous studies that the rise of the thermal difference spectrum does not directly follow the relaxation of the O–D stretch vibration. This rise is somewhat delayed and this delay can be accounted for by letting the relaxation of the O–D stretch vibration proceed through an intermediate state.[39–41] Consequently, we model the isotropic spectra with a three state consecutive model:[40]

$$\Delta\alpha_{\mathrm{iso}}(\omega,t) = \sigma_1(\omega)N_1(0)e^{-k_1 t} + \sigma_3(\omega)\left(N_3(0) + N_1(0)(1 + \frac{k_1 e^{-k_2 t} - k_2 e^{-k_1 t}}{k_2 - k_1})\right) \qquad (3)$$

In this model the excited state (1) with associated spectrum $\sigma_1(\omega)$ relaxes with a rate constant k_1 to the intermediate state (2). This intermediate state is assumed to have the same absorption spectrum as the ground state, meaning that we take $\sigma_2(\omega) = 0$. The intermediate state relaxes with a characteristic rate constant k_2 to the heated end-state (3) with a transient spectrum $\sigma_3(\omega)$. The vibrational population lifetimes corresponding to these rate constants are $\tau_j = 1/k_j$. $N_1(0)$ and $N_3(0)$ represent the initial populations of the excited state and the heated end state, respectively.

The fast vibrational relaxation of the broadband background will result in a significant amount of heat at early times, that is accounted for by taking $N_3(0)$ different from zero. This amount was determined independently by a spectral decomposition of the transient

spectra at early delays into the spectra of the excited state and the heated end state. The population $N_3(0)$ was obtained by extrapolating the obtained values $N_3(t)$ to $t = 0$. For 4 M NaOH (in 4 % D_2O in H_2O) $N_3(0)$ amounts to ~ 0.5, meaning that at this concentration about 50 % of the pump energy excites the broadband O–H background (Figure 5a).

The rate constants and the spectra associated with each state are obtained by fitting the isotropic data $\Delta\alpha_{\mathrm{iso}}(\omega, t)$ over the measured frequency range and delay times >500 fs. In this fit the rate constants are the independent parameters and they are assumed to be constant over the investigated range of frequencies.

From the fit it follows that the vibrational lifetime of the excited state significantly decreases as the concentration of NaOH increases (Figure 4a). These vibrations are located on HOD molecules that are not directly interacting with the hydroxide ions. The vibrations of molecules hydrating the hydroxide ions decay significantly faster. The isotropic lifetime decreases smoothly from $\tau_1 = 1.7 \pm 0.2\,\mathrm{ps}$ ($k_1 = 0.6 \pm 0.1\,\mathrm{ps}^{-1}$) at 0 M to $\tau_1 = 1.0 \pm 0.2\,\mathrm{ps}$ ($k_1 = 1.0 \pm 0.2\,\mathrm{ps}^{-1}$) at 5 M (Figure 5b).

For the complementary system, i.e. the O–H stretch vibration at $3400\,\mathrm{cm}^{-1}$ of HDO molecules in solutions of NaOD in D_2O, we observe similar relaxation dynamics. The excitation shows a fast decaying component with a time constant of $\sim 100\,\mathrm{fs}$ and a slower component with a time constant of $\sim 700\,\mathrm{fs}$. The symmetrical broadening of the associated spectra of the excited O–H oscillators (Figure 3b, $j = 1$) is less pronounced than observed for the O–D stretch vibration at $2500\,\mathrm{cm}^{-1}$ (Figure 3a). This can be explained by the narrower range of frequencies monitored for experiments at $3400\,\mathrm{cm}^{-1}$, due to the narrower probe pulses with respect to the O–H absorption band.

In contrast to the findings for the O–D stretching vibration, the associated spectra of the heated state show only little variation with concentration (Figure 3a, $j = 1$) due to the absence of a concentration-dependent broadband background. The slight variations of σ_3 at $\sim 3400\,\mathrm{cm}^{-1}$ with increasing concentration are most likely due to the appearance of the shoulder in the linear spectra (Figure 1) due to the OH^- stretching vibration.

The experimental transient spectra were modeled with the same kinetic model as for the O–D vibration. As can be seen from the normalized isotropic populations of the excited states, $N_1(t)/N_1(0)$, (Figure 4b) a similar decrease in the isotropic lifetime is observed for the excited O–H oscillators as is observed for the O–D vibrations (see above). The isotropic lifetime decreases smoothly from $\tau_1 = 750 \pm 50\,\mathrm{fs}$ ($k_1 = 1.3 \pm 0.1\,\mathrm{ps}^{-1}$) for a solution of 0 M

NaOD to $\tau_1 = 600 \pm 50\,\mathrm{fs}$ ($k_1 = 1.7 \pm 0.1\,\mathrm{ps}^{-1}$) for a solution of 6 M NaOD (Figure 4b).

3. Anisotropy Results

To obtain the anisotropy dynamics of the excited O–D and O–H stretch vibrations, we need to correct the measured signals for the ingrowing heating signal.[38] To determine the heating signal resulting from the excitation of the broadband $\mathrm{OH}\cdots\mathrm{OH}^-$ background, we measured the transient spectral dynamics of samples without isotopic dilution, i.e. aqueous solutions of NaOH. In these experiments we only excite the O–H stretching band of H_2O molecules solvating OH^- (Figure 1). These experiments confirm that the excitation of these O–H is short lived. The heating of the sample is found to follow subsequent dynamics in which the solutions equilibrate from a local strongly heated state to a homogenously distributed heated state. An important feature of these dynamics is that in the initially formed locally heated state the heat is not distributed isotropically, i.e. the heat effect possesses a residual anisotropy (Figure 6a).[37]

We corrected the transient spectra ($\Delta\alpha_\parallel(\omega,t)$ and $\Delta\alpha_\perp(\omega,t)$) of the O–D stretch vibration for the anisotropic heating effect. Because the heating signal dominates the transient spectra at long delays, this correction affects the resulting $R(t)$ of the excited HOD molecules mainly at $t > 1\,\mathrm{ps}$ (Figure 6a). The resulting anisotropy $R(t)$ decays with a characteristic time constant of $\tau_{\mathrm{or}} \approx 2.4\,\mathrm{ps}$ for all hydroxide concentrations (Figure 6b). This time constant is the same as observed for the O–D vibration of a dilute solution of HDO in H_2O neat water.[23,40,42] This finding indicates that the orientational dynamics of water molecules outside the first hydration shell of the OH^- ion are unaffected by the alkaline environment.

C. Terahertz spectroscopy

Figure 7a shows that the measured permittivity, ε', increases with increasing concentration of NaOH and KOH. The constant increase over the entire investigated frequency range likely originates from the enhancement or appearance of higher frequency modes ($\nu > 1.2\,\mathrm{THz}$). Similar effects have been observed recently for aqueous electrolyte solutions.[43,44] Secondly, a pronounced decrease in the dielectric loss, ε'', is observed. At THz frequencies the main contribution to ε'' stems from the dominant water orientational

relaxation mode centered at 20 GHz. Hence the decrease indicates a substantial decrease in the number of water molecules engaged in this reorientation.

For aqueous electrolyte solutions it has been shown previously[45] that three different kind of water species may be distinguished using THz spectroscopy. In the first place, there are water molecules which are not affected by the presence of the ions. Clearly, the THz spectrum of these water molecules will remain unchanged. Secondly, there are water molecules that are tightly bound in the hydration shell around the ions. These no longer contribute to the dielectric spectra, because their dipole moments cancel out due to the spherical symmetry hydration shell. While not directly affected by the presence of the ions, a third fraction of water molecules is affected by the translational motion of the ions. The ions are accelerated by the externally applied alternating THz electric field, and give rise to changes in the local electric field, thereby affecting the reorientation of neighboring water molecules in their vicinity. As a result, these water molecules do not contribute to the observed relaxation mode - an effect known as kinetic depolarization. Hence, both water molecules directly bound to ions, and those affected by the motion of ions result in a depolarization, i.e. a decrease of the relaxation strength as already apparent from the data shown in Figure 7.

1. Data Analysis

To quantify the number of water molecules that remain unaffected by the presence of NaOH and KOH, we need to determine the overall amplitude of the rotational relaxation mode by fitting an appropriate model to the experimental spectra. Previous GHz dielectric relaxation studies have shown that the addition of NaOH leads to a symmetrical broadening of the dominant relaxation mode at 20 GHz, while keeping the relaxation time (i.e. the position of the maximum in ε'') rather constant.[46] The broadening of the mode can be described by a Cole-Cole equation representing a distribution of relaxation times.[46] Following these observations we modeled the THz spectra, $\hat{\varepsilon}(\nu)$ with a sum of a lower-frequency Cole-Cole (CC) equation for the main relaxation mode and a higher frequency Debye mode representing the fast mode[22]

$$\hat{\varepsilon}(\nu) = \frac{S_{\mathrm{CC}}}{1 + (2\pi\nu \mathrm{i}\tau_{\mathrm{CC}})^{(1-\alpha_{\mathrm{CC}})}} + \frac{S_{\mathrm{f}}}{1 + 2\pi\nu \mathrm{i}\tau_{\mathrm{f}}} + \varepsilon_{\infty} \tag{4}$$

where τ_j and S_j represent the relaxation times (peak positions) and relaxation strengths

(amplitudes) of both modes, respectively. The Cole-Cole parameter α_{CC} was inter- or extrapolated from values in the literature to the concentrations of the present study.[46] Following previous work,[15] τ_{CC} was fixed to the value obtained from the reference sample (pure water, see experimental section) using the known static permittivity of water.[47] The static permittivity of the sample, ε^{stat}, corresponds to the sum of the amplitudes and the infinite frequency permittivity, ε_∞ ($\varepsilon^{stat} = \lim_{\nu\to 0}\varepsilon' = S_{CC} + S_f + \varepsilon_\infty$). Using this approach, we obtain the amplitude of the rotational relaxation mode, S_{CC}.

The value of S_{CC} can be translated to the concentration of unaffected water molecules using the Cavell equation.[48,49] This equation relates the relaxation amplitude S_{CC}, to the apparent concentration of water, c_{app,H_2O} as detected with THz spectroscopy:

$$\frac{2\varepsilon^{stat}+1}{\varepsilon^{stat}} \cdot S_{CC} = \frac{N_A\, c_{app,H_2O}}{k_B\, T \varepsilon_0} \cdot \mu_{eff}^2 \tag{5}$$

where ε^{stat} is the static permittivity of the sample, N_A and k_B are the Avogadro and Boltzmann constant, respectively and T is the thermodynamic temperature. μ_{eff} is the effective dipole moment of the relaxing species. μ_{eff} was assumed to be constant and the same as for neat water.[50]

The major fraction of water molecules that do not contribute to the observed relaxation mode corresponds to H_2O molecules that are affected by charge transport. This kinetic depolarization effect depends on the mobility of the ions in the solutions (i.e. the conductivity κ), the dielectric function that determines the screening of the local electric field and on the dynamics of the water molecules. Its contribution can be calculated with the following equation:[45,51,52]

$$\Delta S_{kd} = \frac{2}{3}\frac{\varepsilon_{stat}^{H_2O} - \varepsilon_\infty^{H_2O}}{\varepsilon_{stat}^{H_2O}}\frac{\tau^{H_2O}}{\varepsilon_0} \cdot \kappa \tag{6}$$

where $\varepsilon_\infty^{H_2O}$ is the infinite frequency permittivity of neat water and τ^{H_2O} is the relaxation time of water.

Inserting ΔS_{kd}, into eq 5 gives the number of water molecules that are involved in the charge transport of the ions as a response of the ions to the external electric field, c_{kd,H_2O}.[15] The number of water molecules per NaOH/KOH ion pair, $Z_{kd} = c_{kd,H_2O}/c$ is displayed in Figure 8a. Z_{kd} shows a smooth decrease from ~ 9 water molecules for dilute solutions to ~ 5 at $c = 5\,M$. The difference between NaOH and KOH solutions can be traced back to

the higher mobility of K^+ compared to Na^+ in water.[1]

The remaining fraction of water molecules that do not show up in the terahertz spectra corresponds to irrotational bonding molecules, i.e. water molecules in a rigid hydration shell of an ion that do not respond to the alternating electric field. The comparison of $c_{\mathrm{kd,H_2O}} + c_{\mathrm{app,H_2O}}$, to the analytical water concentration, $c_{\mathrm{H_2O}}$, that decreases with concentration due to the dilution effect, gives the number of water molecules within the rigid hydration shell around the ion. The irrotationally bound hydration number, $Z_{\mathrm{ib}} = (c_{\mathrm{H_2O}} - c_{\mathrm{kd,H_2O}} - c_{\mathrm{app,H_2O}})/c$ so obtained is roughly constant over the investigated concentration range (Figure 8b). For NaOH an average value of $Z_{\mathrm{ib}} \approx 2.5$ which is slightly lower than the ~ 4.5 water molecules found for Na^+ ion in NaCl.[45]

To clarify the influence of the hydration shell around the cation, the hydration number of NaOH is compared to that of aqueous solutions of KOH. The results for aqueous solutions of KOH yield a negligible (and even slightly negative) number of bound water molecules for aqueous solutions of KOH (Figure 8b). This finding is in accordance with a neutron diffraction study[5] that indicates no radial alignment of water dipoles around K^+ in contrast to Na^+. It also agrees with an earlier dielectric relaxation study in which no irrotationally bound water was detected around K^+.[53]

The difference between the present Z_{ib} values and results obtained for the corresponding chloride salts[45,53] can be explained by the presence of the hydroxide ion. Due to its symmetry, OH^-, has a dipole moment itself. The addition of an OH^- ion, that is incorporated into the three dimensional hydrogen bonded structure will contribute to the overall dielectric response.[22] Hence, the effective number of water dipoles in the hydrogen-bonded structure, can be higher than the analytical water concentration, $c_{\mathrm{H_2O}}$, which can explain the observed difference between the hydration numbers for the hydroxide and the corresponding chloride salt. There are thus no indications for the formation of a rigid hydration shell around the hydroxide ion.[54]

The amplitude of the fast Debye mode increases from $S_{\mathrm{D}} = 1.3$ at 0 M to ≈ 2 at 4 M for both NaOH and KOH. This observation is in line with earlier findings for solutions of hydrophobes[26] and lipids[21] and indicates an enhanced number of undercoordinated water molecules. The relaxation time of this mode remains rather constant ($\tau_{\mathrm{D}} \approx 100$ fs).

IV. DISCUSSION

Figure 6b shows that the decay of the anisotropy of excited O–D oscillators is unaffected by the presence of NaOH (Figure 6b). At this point it should be reminded that this anisotropy represents the reorientation of O–D groups of HDO molecules that are not directly interacting with the OH^- ion. For OD groups that are directly interacting with the OH^- ion, the O–D stretch vibration has a different (redshifted) spectral response and a very short vibrational relaxation time, so that the contribution of these oscillators vanishes at delay times >1 ps. The results of Figure 6b imply that the hydroxide ion does not have a long-range effect on the hydrogen-bond structure of the liquid. This result agrees with the results of a previous dielectric relaxation study in which it was found that the time constant τ_{CC} of the main relaxation mode is not affected by the presence of NaOH.[46] For the proton in water a similar observation was made: water molecules outside the first hydration shell of the proton showed the same reorientation time constant as the molecules in bulk liquid water.[12]

Interestingly, the vibrational lifetime of the O–D and O–H vibrations is observed to decrease with increasing concentration NaOH/NaOD (Figures 4 & 5b). This decrease in lifetime is likely the result of the presence of the OH^-/OD^- ions, because the effect of cations, like Na^+ and K^+, on vibrational lifetimes is found to be very small.[55,56] As can be seen in Figure 5b, the concentration dependencies of the decay rates, k_1, of O–H and O–D are quite similar.

As both the linear absorption spectrum and the reorientation dynamics of OH groups outside the first hydration shell are observed to be unaffected by the presence of the OH/OD group, the acceleration of the vibrational energy relaxation cannot be ascribed to a change in the strength of the hydrogen-bond interaction. The acceleration can also not be ascribed to Förster energy transfer from the excited O–D/O–H vibration to H_2O/D_2O molecules hydrating the OH^-/OD^- ion. This type of Förster energy transfer has been observed for the proton in water.[12] In this latter study the O–D stretch vibration of HDO was observed to show an additional distinctly non-exponential decay that became faster with increasing proton concentration. This additional decay finds its origin in vibrational Förster energy transfer to the background of water molecules hydrating the proton.[12] For the complementary system, i.e. the O–H stretch vibration and vibrations of D_2O molecules hydrating D^+, no

acceleration of the vibrational relaxation was observed, because the O–H vibration is not in resonance with the D_2O molecules hydrating D^+. In the present study we observe similar accelerations for the O–D and O–H stretch vibration outside the first hydration shells of OH^- and OD^-, respectively. However only the O–D vibration will be in resonance with the H_2O molecules hydrating OH^-, thereby excluding Förster energy transfer as the dominant mechanism of the observed acceleration. Thus, it appears that the dipolar coupling of the O–D stretch vibration with the broadband background of the O–H stretch vibrations of H_2O molecules hydrating H^+ is much weaker for alkaline solutions than for acidic solutions. This notion agrees with the lower infrared absorption cross-section of O–H$\cdots$$OH^-$ compared to O–H$\cdots$$H^+$.

We do not find any evidence for a double exponential decay of the vibrational relaxation of the O–D and O–H stretch vibrations. Hence, distinct subensembles of OD/OH groups with distinct, different lifetimes of the stretching vibrations in the vicinity of OH^- or OD^- can be excluded. The acceleration of the vibrational relaxation of the O–D and O–H stretch vibration likely finds its origin in the fluctuations in the charge distribution and structure of the hydration structure around the OH^- ion. These charge and structure fluctuations are intimitately connected, meaning that structural dynamics around OH^- ion will induce charge fluctuations and vice versa. The rate of vibrational energy relaxation is not only determined by the strength of the anharmonic coupling between the excited vibration and the energy-accepting modes, but also by the time scale and magnitude of the fluctuations of the energy levels of these modes. The fluctuations in charge resulting from the exchange of protons between the hydroxide ion and the water molecules in its first hydration shell, will induce strong fluctuations in the energies of the vibrations of nearby water molecules. These fluctuations will help in making the energy transfer from the excited O–D/O–H to the accepting modes resonant, thereby accelerating the vibrational relaxation.

More specifically, Figure 9 depicts the possible proton transfer events together with the O–D oscillators absorbing at $\sim$2500 cm^{-1} of which the vibrational relaxation will be affected by proton transfer events. O–D oscillator (a) belongs to an HDO molecule in the first hydration shell, but the probed oscillator points away from the hydroxide ion. In the case of proton transfer process (1), the O–H group of the HDO molecule is no longer hydrating a hydroxide ion but an H_2O molecule. This will induce a strong change of the donated hydrogen bond and thus of the frequencies of the stretch vibrations, the bending mode

and the librational modes of the HDO molecule. These fluctuations may enable a quick relaxation of O–D vibration (a). For O–D oscillator (b), proton transfer process (1) implies that the O–D group shifts from the second hydration shell to the third hydration shell. This transition will also lead to fluctuations of the vibrational frequencies of the HDO molecule to which O–D belongs. Clearly these frequency changes will be much smaller than for O–D oscillator (a), but could still be sufficient to enable vibrational relaxation. In the case of proton transfer process (2), O–D oscillator (a) becomes the stretch vibration of an OD^- ion. This transfer is accompanied by a change in frequency and cross-section of the O–D stretch vibration, which will lead to a vanishing of this oscillator from the observed bleaching signal at $\sim$2500 cm^{-1}. Thereby this transfer contributes to the decay of this signal. For O–D oscillator (b), proton transfer process (2) implies that this oscillator turns into an oscillator solvating a hydroxide ion. This will lead to a large change in frequency and thus to a vanishing of the contribution of this oscillator to the bleaching signal at $\sim$2500 cm^{-1}. Moreover, the vibrational relaxation of O–D oscillators directly hydrating the hydroxide ion is very short, on a 120-160 fs time scale[3,4], meaning that proton transfer process (2) effectively induces a direct relaxation of O–D oscillator (b).

The exchange between the hydroxide ion and water due to proton transfer has recently been observed with two-dimensional femtosecond infrared spectroscopy.[13] In that study it was found that this exchange takes places on a relatively long time scale with a lower boundary of 3 ps. This long time constant is the result of the relatively slow solvation of the newly formed hydroxide ion. In view of this finding, it seems quite likely that the acceleration of the vibrational relaxation does not require the completed solvation of the newly formed hydroxide ion. Instead, the fluctuations of the average position of the proton between the oxygen atom of the hydroxide ion and the oxygen atoms of the water molecules in the first hydration shell, already suffice to modulate the energies of the HDO molecules containing O–D oscillators (a) and (b). Hence, the charge fluctuations can induce vibrational relaxation of these oscillators without the necessity of achieving a completed proton transfer.

The above mentioned four combinations of oscillators and proton transfer processes all contribute to the acceleration of the relaxation of the O–D/O–H oscillators. Hence the presence of the hydroxide ion enables the rapid relaxation of O–D/O–H oscillators that are close to the hydroxide ion. The rate of this channel is determined by the time scale of the fluctuations of the proton charge, and its contribution to the overall averaged relaxation is

determined by the fraction of water that is found in the first and second hydration shell. This fraction increases with the hydroxide concentration. This picture is in line with the concentration dependence of the relaxation shown in Figure 5b, and the observation that the acceleration is quite similar for the O–D and O–H stretch vibration. It is also consistent with the observation of a single exponential vibrational relaxation (i.e. the absence of distinctively different subensembles of excited molecules in proximity to the hydroxide ion and and of bulk HDO molecules). The variation of the single exponential decay with concentration of NaOH suggests that the observed decay rate, k_1, can be related to two effects. The observed rate for the single-exponential decay, k_1, for O–D and O–H at different concentrations is composed of a first order kinetic term, k_1°, that corresponds to the relaxation in neat water and a second order term, $k_{\mathrm{OH^-}} c_{\mathrm{OH^-}}$, associated with the decay due to fluctuations caused by the hydroxide ion ($k_1 = k_1^{\circ} + k_{\mathrm{OH^-}} c_{\mathrm{OH^-}}$). Only the second order term is affected by the OH^-/OD^- concentration. Applying this simple model to the data results in a rate enhancement term amounting to $k_{\mathrm{OH^-}} = 50 \pm 9\,\mathrm{L\,mol^{-1}\,fs^{-1}}$ for the concentration dependence of both O-D and O-H vibration with concentration.

An interesting question is why proton/deuteron transfer affects the vibrational relaxation of the hydration shells of the hydroxide ion but not of the hydration shell of the proton. The latter is apparent from the fact that for the O–H stretch vibration outside the first hydration shell of D^+ no acceleration was observed.[12] This difference in the effect of proton/deuteron transfer on the relaxation can be explained from the specific hydration structures of the proton and the hydroxide ion. For the proton, the water molecules in the first hydration shell are forming Zundel ($H_5O_2^+$) or Eigen ($H_9O_4^+$) cations. The stretch vibrations of these structures are strongly redshifted with respect to the O–D and O–H stretch vibrations of HDO and have different (shorter) vibrational relaxation rates than these vibrations.[57] Hence, the first hydration shell of the proton will hardly contribute to the signal of the O–D at $\sim$2500 $\mathrm{cm^{-1}}$ and that of the O–H at $\sim$3400 $\mathrm{cm^{-1}}$. The water molecules in the second hydration shell of the proton will absorb at 2500/3400 $\mathrm{cm^{-1}}$. These water molecules accept hydrogen bonds at their oxygen atoms from the water molecules in the first hydration shell. Proton transfer will affect the strength of this hydrogen bond, but the effect of a change in an accepted hydrogen bond on the vibrational frequencies will be small. For the hydroxide ion, the signals of O–D/O–H oscillators (a) (first hydration shell) and (b) (second hydration shell) will contribute to the signal at 2500/3400 $\mathrm{cm^{-1}}$. These O–D/O–H oscillators belong

to HDO molecules that *donate* a hydrogen bond to the hydroxide ion or to a water molecule in the first hydration shell. Proton transfer from a water molecule in the first hydration shell to the hydroxide ion will strongly affect the strength of this hydrogen bond. As this is a donated hydrogen bond, this will lead to a large change of the frequencies of the vibrations (librations, bending mode, stretch vibrations) of the water molecule. Hence, in the latter case the proton/deuteron transfer affects the energy matching of the excited vibration and the accepting modes, and thereby the rate of vibrational relaxation.

The present dielectric relaxation experiments using terahertz time-domain spectroscopy show that only the sodium ion has a rigid hydration shell with irrotationally bound water molecules (Figure 8b), while for K^+ a depolarization due to interaction of water molecules with the cation cannot be detected. This finding is consistent with the lower charge density of K^+ compared to Na^+ and with earlier dielectric measurements.[45,53] For both aqueous solutions of NaOH and KOH no slow water molecules in the vicinity of OH^- are observed.[54] This appears to be in contrast with the previous observation of four tightly bound water molecules in the hydration shell of H^+.[15] However, cations like the proton can lock water dipoles, that are monitored in dielectric relaxation experiments, much more efficiently than anions that form hydrogen bonds with the O–H vector pointing towards the anion.[17,28] Consequently, in the hydration shell of an anion, one of the O–H groups of the hydrating water molecules can be tightly bound to the OH^- ion, but the dipole vector of these water molecules can still possess a significant rotational freedom.[17,58]

The present results indicate that the transport of the hydroxide ion at $c = 1\,\mathrm{M}$ involves the rearrangement of $Z_{\mathrm{kd}} \sim 9$ and $Z_{\mathrm{kd}} \sim 8$ water molecules for KOH and NaOH, respectively (Figure 8a). This number includes water molecules involved in the translation of both the OH^- ion and the cation (K^+ or Na^+). The contribution can be split into single ion contributions on the basis of the mobilities of the single ions assuming transference numbers from literature.[1] According to this approach ~ 7 water molecules are affected by the transfer of the charge of the hydroxide ion at 1 M. This number of water molecules that accompany the charge transport is significantly lower than for the H^+ ion ($Z_{\mathrm{kd}} \approx 15$).[15] The difference between the proton and the hydroxide ion indicates that the structural diffusion mechanisms of the two ions are significantly different. Hence, this finding supports the notion that aqueous OH^- and H^+ solutions are not each others mirror images, neither in hydration structure nor in transport mechanism, as previously proposed.[11]

V. CONCLUDING REMARKS

We studied the vibrational relaxation dynamics and orientational dynamics of water molecules solvating hydroxide ions with polarization-resolved femtosecond vibrational spectroscopy. We investigated the dynamics of the O–D stretch vibration of HDO molecules in OH^-/H_2O solutions and the dynamics of the O–H stretch vibration of HDO molecules in OD^-/D_2O solutions. We also studied the orientational dynamics of water molecules in solutions of NaOH and KOH in H_2O using transient THz dielectric relaxation spectroscopy.

We observe that the hydroxide ion induces an acceleration of the vibrational relaxation of the O–D/O–H groups that are not directly interacting with the hydroxide ions. The relaxation rate for O–D of HDO molecules outside the first hydration shell of OH^- increases from $0.60\pm0.06\,ps^{-1}$ for HDO:H_2O to $1.0\pm0.1\,ps^{-1}$ for a solution of 5 M NaOH in HDO:H_2O. For the O–H of HDO molecules outside the first hydration shell of OD^- we observe a similar acceleration from $1.3\pm0.1\,ps^{-1}$ for HDO:D_2O to $1.7\pm0.1\,ps^{-1}$ for a solution of 6 M NaOD in HDO:D_2O. The magnitude of the acceleration is similar for the two complementary systems, and can be well explained from the occurrence of proton/deuteron transfer events between the water molecules in the first hydration shell and the hydroxide ion. The proton/deuteron transfer induces a strong modulation of the vibrational frequencies of the vibrations (librations, bending mode, stretch modes) of the water molecules in the first and second hydration shell, thus enabling a fast vibrational relaxation of the excited O–D/O–H stretch vibration.

The reorientation dynamics of the O–D vibration of HDO molecules outside the first hydration shell of OH^- show a time constant of 2.5±0.2 ps, similar to bulk water and independent of the hydroxide concentration. This finding shows that the hydroxide ion does not have a long-range effect on the hydrogen-bond network of liquid water. This finding agrees with the results of previous dielectric relaxation studies in which it was found that the time constant of the main bulk-like relaxation component of water is not affected by the addition of hydroxide salts.

The THz dielectric relaxation studies showed that the hydration shell of the hydroxide ion does not contain water molecules for which the orientational mobility of the dipole vector is strongly reduced. This finding is in line with previous work showing that cations like the proton are much more effective than anions in locking the dipoles of hydrating water molecules. We also find that the transfer of the hydroxide ion involves the motion of ∼7

surrounding water molecules at 1 M. This number is significantly lower than the number of water molecules involved in the transfer of the proton, thus indicating that the hydroxide ion and the proton show significantly different transfer mechanisms in liquid water.

Acknowledgment

This work is part of the research program of the *Foundation for Fundamental Research on Matter (FOM)*, which is part of the *Netherlands Organisation for Scientific Research (NWO)*. JH thanks the *Deutsche Forschungsgemeinschaft* (DFG) for funding through the award of a research fellowship.

[1] Y. Marcus, *Ion Properties* (Marcel Dekker, New York, 1997).

[2] C. J. T. de Grotthuss, Ann. Chim. **58**, 54 (1806).

[3] A. T. Roberts, P. B. Petersen, K. Ramasesha, A. Tokmakoff, I. S. Ufimtsev, and T. J. Martinez, Proc. Natl. Acad. Sci. U.S.A. **106**, 15154 (2009).

[4] H.-K. Nienhuys, A. J. Lock, R. A. van Santen, and H. J. Bakker, J. Chem. Phys. **117**, 8021 (2002).

[5] S. Imberti, A. Botti, F. Bruni, G. Cappa, M. A. Ricci, and A. K. Soper, J. Chem. Phys. **122**, 194509 (2005).

[6] C. D. Cappa, J. D. Smith, B. M. Messer, R. C. Cohen, and R. J. Saykally, J. Phys. Chem. A **111**, 4776 (2007).

[7] E. F. Aziz, N. Ottosson, M. Faubel, I. V. Hertel, and B. Winter, Nature **455**, 89 (2008).

[8] T. Megyes, S. Bálint, T. Grósz, T. Radnai, I. Bakó, and P. Sipos, J. Chem. Phys. **128**, 044501 (2008).

[9] N. Agmon, Chem. Phys. Lett. **319**, 247 (2000).

[10] D. Asthagiri, L. R. Pratt, L. D. Kress, and M. A. Gomez, Proc. Natl. Acad. Sci. U.S.A. **101**, 7229 (2004).

[11] D. Marx, A. Chandra, and M. E. Tuckerman, Chem. Rev. **110**, 2174 (2010).

[12] R. L. A. Timmer, K.-J. Tielrooij, and H. J. Bakker, J. Chem. Phys. **132**, 194504 (2010).

[13] S. T. Roberts, K. Ramasesha, P. B. Petersen, A. Mandal, and A. Tokmakoff, J. Phys. Chem. A **115**, 3957 (2011).

[14] H. N. Chen, G. A. Voth, and N. Agmon, J. Phys. Chem. B **114**, 333 (2010).

[15] K. J. Tielrooij, R. L. A. Timmer, H. J. Bakker, and M. Bonn, Phys. Rev. Lett. **102**, 198303 (2009).

[16] S. E. McLain, S. Imberti, and A. K. Soper, Phys. Rev. B **74**, 094201 (2006).

[17] K. J. Tielrooij, N. Garcia-Araez, M. Bonn, and H. J. Bakker, Science **328**, 1006 (2010).

[18] H. J. Bakker, Y. L. A. Rezus, and R. L. A. Timmer, J. Phys. Chem. A **112**, 112 (2008).

[19] J. Ahn, V. Efimov, R. D. Averitt, and A. J. Taylor, Opt. Express **11**, 1861 (2003).

[20] E. Knoesel, M. Bonn, J. Shan, F. Wang, and T. F. Heinz, J. Chem. Phys. **121**, 394 (2004).

[21] K. J. Tielrooij, D. Paparo, L. Piatkowski, H. J. Bakker, and M. Bonn, Biophys. J. **97**, 2484

(2009).

[22] T. Fukasawa, T. Sato, J. Watanabe, Y. Hama, W. Kunz, and R. Buchner, Phys. Rev. Lett. **95**, 197802 (2005).

[23] K. J. Tielrooij, C. Petersen, Y. L. A. Rezus, and H. J. Bakker, Chem. Phys. Lett. **471**, 71 (2009).

[24] J. Hunger, A. Stoppa, A. Thoman, M. Walther, and R. Buchner, Chem. Phys. Lett. **471**, 85 (2009).

[25] D. Laage and J. T. Hynes, Science **311**, 832 (2006).

[26] K. J. Tielrooij, J. Hunger, R. Buchner, M. Bonn, and H. J. Bakker, J. Am. Chem. Soc. **132**, 15671 (2010).

[27] D. A. Turton, J. Hunger, G. Hefter, R. Buchner, and K. Wynne, J. Chem. Phys. **128**, 161102 (2008).

[28] R. Buchner and G. Hefter, Phys. Chem. Chem. Phys. **11**, 8954 (2009).

[29] L. S. Darken and H. F. Meier, J. Am. Chem. Soc. **64**, 621 (1942).

[30] H. J. de Wane and W. J. Hamer, Sci. Tech. Aerosp. Rep. **7**, 28 (1969).

[31] A. H. Roux, G. Perron, and J. E. Desnoyers, Can. J. Chem. **62**, 878 (1984).

[32] J. Tamás, Acta Chim. Acad. Sci. Hung. **40**, 117 (1964).

[33] N. B. Librovich, V. P. Sakun, and N. D. Sokolov, Chem. Phys. **39**, 351 (1979).

[34] M. Śmiechowski and J. Stangret, J. Phys. Chem. A **111**, 2889 (2007).

[35] Y. Millo, Y. Raichlin, and A. Katzir, Appl. Spectroscopy **59**, 460 (2005).

[36] H. J. Bakker and J. L. Skinner, Chem. Rev. **110**, 4148 (2010).

[37] L. Liu and H. J. Bakker, unpublished results.

[38] Y. L. A. Rezus and H. J. Bakker, J. Chem. Phys. **125**, 144512 (2006).

[39] T. Steinel, J. B. Asbury, J. Zheng, and M. D. Fayer, J. Phys. Chem. A **108**, 10957 (2004).

[40] Y. L. Rezus and H. J. Bakker, J. Chem. Phys. **123**, 114502 (2005).

[41] R. Timmer and H. J. Bakker, J. Chem. Phys. **126**, 154507 (2007).

[42] D. E. Moilanen, E. E. Fenn, Y. S. Lin, J. L. Skinner, B. Bagchi, and M. D. Fayer, Proc. Natl. Acad. Sci. U.S.A. **105**, 5295 (2008).

[43] I. A. Heisler, K. Mazur, and S. R. Meech, J. Phys. Chem. B **115**, 1863 (2011).

[44] D. A. Schmidt, O. Birer, S. Funkner, B. P. Born, R. Gnanasekaran, G. W. Schwaab, D. M. Leitner, and M. Havenith, J. Am. Chem. Soc. **131**, 18512 (2009).

[45] R. Buchner, G. Hefter, and P. M. May, J. Phys. Chem. A **103**, 1 (1999).

[46] R. Buchner, G. Hefter, P. M. May, and P. Sipos, J. Phys. Chem. B **103**, 11186 (1999).

[47] D. P. Fernández, A. R. H. Goodwin, E. W. Lemmon, J. M. H. Levelt Sengers, and R. C. Williams, J. Phys. Chem. Ref. Data **26**, 1125 (1997).

[48] E. A. S. Cavell, P. C. Knight, and M. A. Sheikh, Trans. Faraday Soc. **67**, 2225 (1971).

[49] J. Hunger, A. Stoppa, R. Buchner, and G. Hefter, J. Phys. Chem. B **113**, 9527 (2009).

[50] J. Hunger, Ph.D. thesis, Regensburg (2009).

[51] J. B. Hubbard and L. Onsager, J. Chem. Phys. **67**, 4850 (1977).

[52] J. B. Hubbard, J. Chem. Phys. **68**, 1649 (1978).

[53] T. Chen, G. Hefter, and R. Buchner, J. Phys. Chem. A **107**, 4025 (2003).

[54] Note that Buchner *et al*[46] suggested that the OH^- ion does not contribute to the kinetic depolarisation due to the different transport mechanism of the hydroxide ions compared to conventional anions. Assuming no influence of the local field of OH^- generated by translation of the ion on the neighboring water molecules, their analysis yielded a rigid hydration shell around the hydroxide ion as well.[46].

[55] H. J. Bakker, Chem. Rev. **108**, 1456 (2008).

[56] M. F. Kropman and H. J. Bakker, Chem. Phys. Lett. **370**, 741 (2003).

[57] S. Woutersen and H. J. Bakker, Phys. Rev. Lett. **96**, 138305 (2006).

[58] R. Buchner, Pure Appl. Chem. **80**, 1239 (2008).

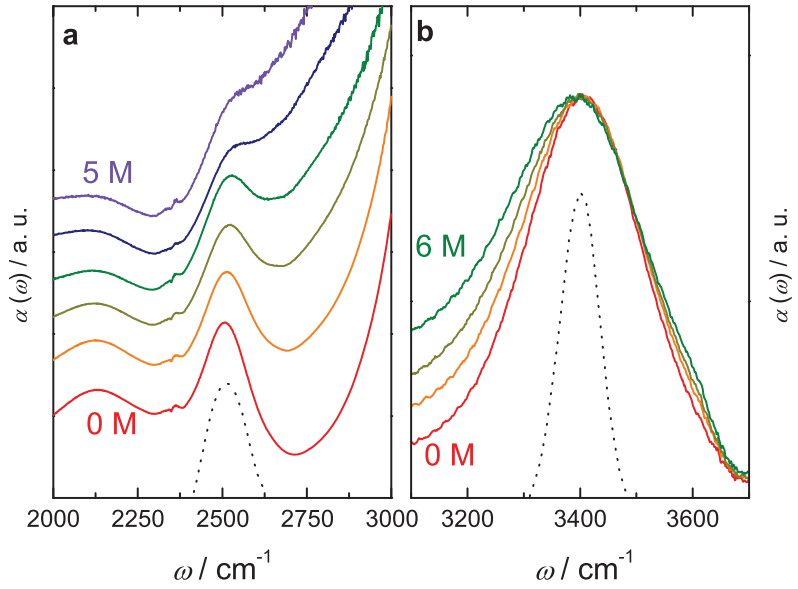

FIG. 1: (**a**) Linear infrared spectra, $\alpha(\omega)$ of solutions of 4 % H_2O and 0, 2, 4 and 6 M NaOD in D_2O, in the frequency region of the O–H stretch vibration. (**b**) Linear infrared spectra of solutions of 4 % D_2O and 0, 1, 2, 3, 4, and 5 M NaOH in H_2O, in the frequency region of the O–H stretch vibration.

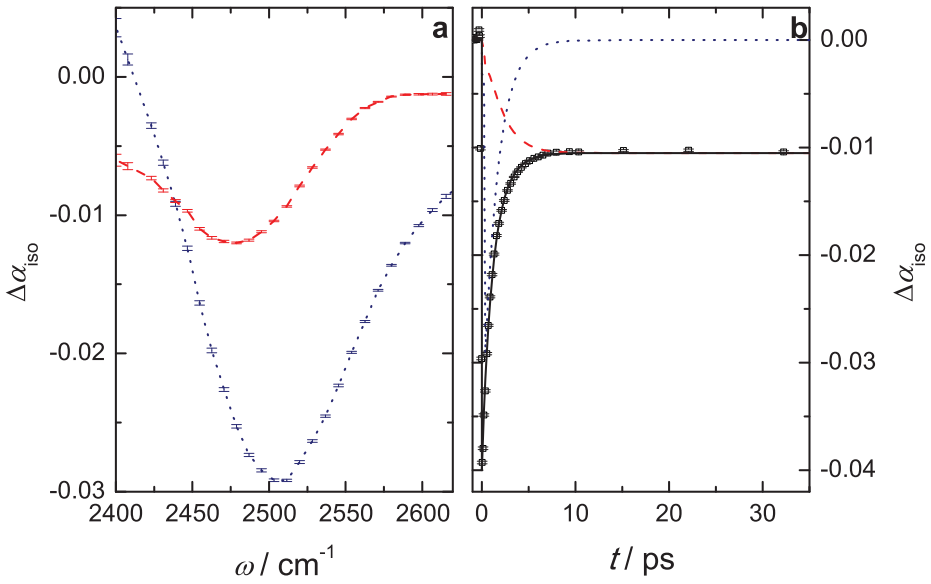

FIG. 2: (**a**) Measured transient absorbtion spectra, $\Delta\alpha_{\mathrm{iso}}(\omega)$ shortly after excitation ($t = 500\,\mathrm{fs}$) representing excited O–D oscillators (solid line) and at long delay ($t = 100\,\mathrm{ps}$) corresponding to the heated end state (dashed line) for a solution of 4 % D_2O and 1.5 M NaOH in H_2O. (**b**) Isotropic transient absorption signal $\Delta\alpha_{\mathrm{iso}}(t)$ at $\omega = 2503\,\mathrm{cm}^{-1}$. The symbols represent the experimental data and the solid line represents the fit with the kinetic model (eq 3, see text). The dashed and the dotted line represent the contributions of the excited state of the O–D oscillators and the heated end state, respectively.

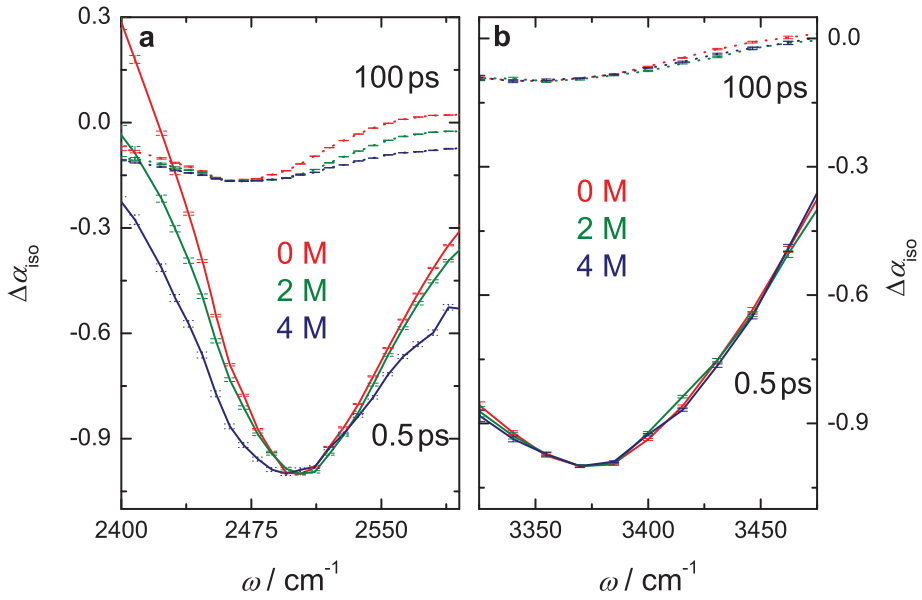

FIG. 3: Transient absorption spectra, $\Delta\alpha_{\mathrm{iso}}(\omega)$ at $t = 0.5\,\mathrm{fs}$ where the excitation is dominating and at long delays ($t = 100\,\mathrm{ps}$) corresponding to thermal difference spectra. Spectra are shown for three concentrations at (**a**) the O–D stretching vibration (0 M: solid line; 2 M: dashed line; 4 M: dotted line) and (**b**) the O–H stretching vibration (0 M: solid line; 2 M: dashed line; 4 M: dotted line).

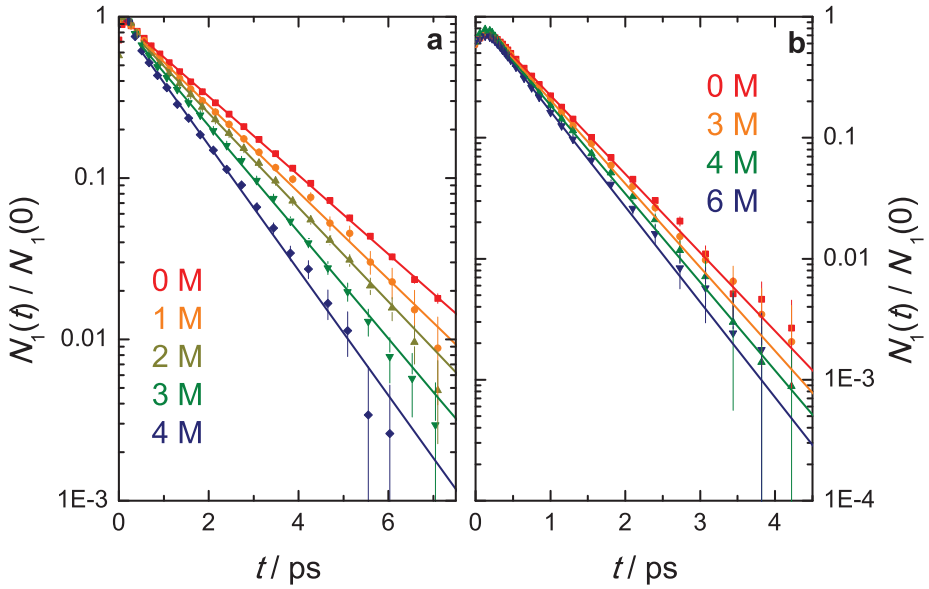

FIG. 4: The normalized populations of the excited state, $N_1(t)/N_1(0)$ as a function of delay time for (**a**) solutions of 4 % D_2O and different concentrations of NaOH in H_2O, and (**b**) solutions of 4 % H_2O and different concentrations of NaOD in D_2O. The symbols correspond to the experimental data corrected for the heating effect (see text), and the lines represent fits with a single exponential decay with rate constant k_1.

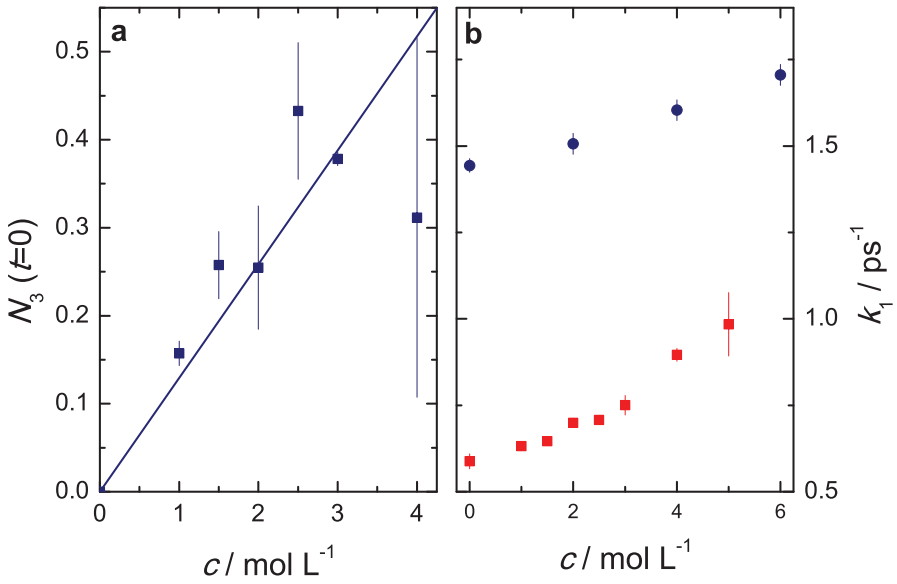

FIG. 5: (**a**) The relative population of the heated end state at $t = 0$ as a function of concentration. These populations are extracted from the spectral decomposition of the transient spectra measured at early delay times (see text). The error bars are determined from the variation of the relative population over different experiments. The solid line corresponds to a linear fit. (**b**) The rate constants k_1 of the relaxation of the excited state as a function of concentration NaOD/NaOH for solutions of 4 % D_2O and different concentrations NaOH in H_2O (■) and solutions of 4 % H_2O and different concentrations NaOD in D_2O (●).

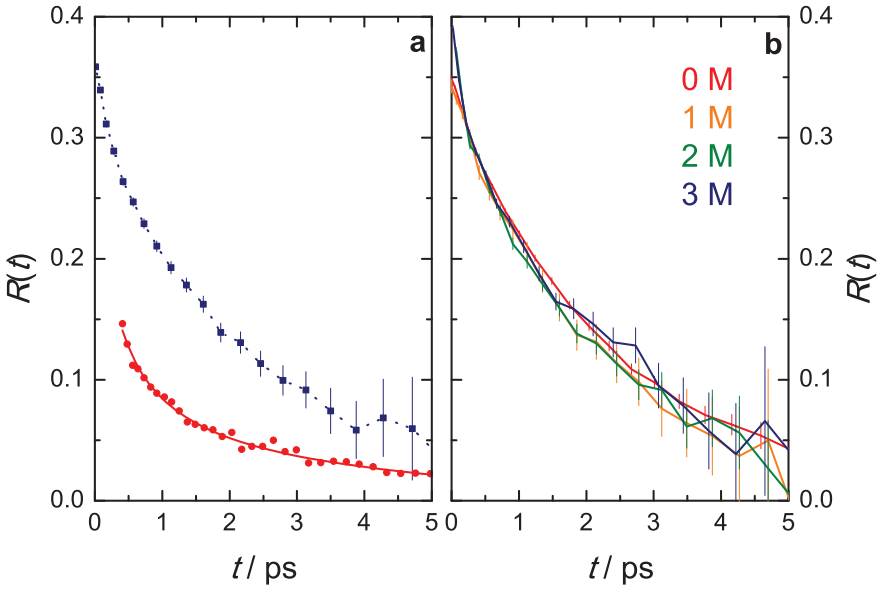

FIG. 6: (**a**) Anisotropy $R(t)$ for the O–D vibration of HDO molecules as a function of delay time for a solution of 2.5 M NaOH in H_2O (■) corrected for the anisotropy in the heating signal. Also shown is the anisotropy of the heating signal that results from the excitation of the broadband background of O–H oscillators of H_2O molecules solvating OH^- (○).[37] (**b**) The anisotropy $R(t)$ of the O–D vibration of HDO molecules as a function of delay time for solutions of 0 M (solid), 1 M (dashed), 2 M (dotted), and 3 M (dashed dotted) NaOH in H_2O. The anisotropy signals are corrected for the anisotropic heating signal.

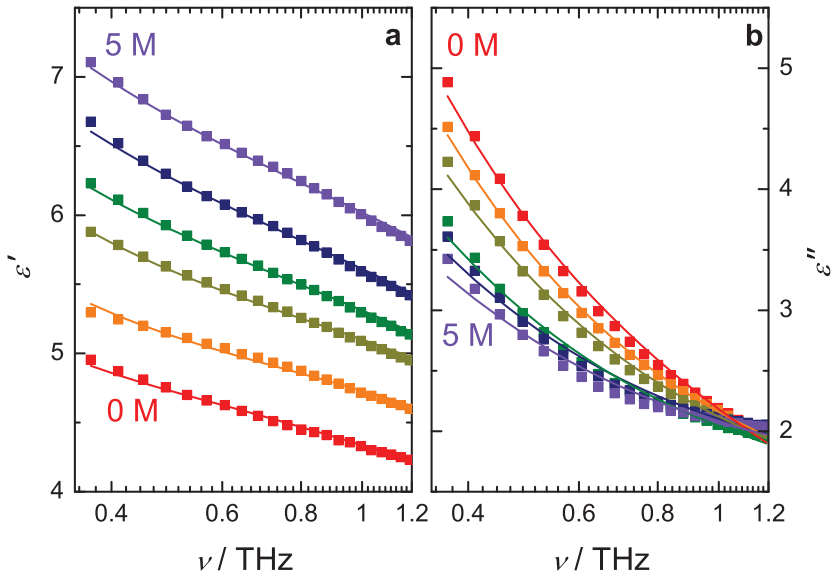

FIG. 7: (**a**) Dielectric permittivity, $\varepsilon'(\nu)$, and (**b**) dielectric loss, $\varepsilon''(\nu)$, at THz frequencies for solutions of different concentrations of NaOH in H_2O. The symbols correspond to the experimental data, the lines represent fits to the data with eq. (4).

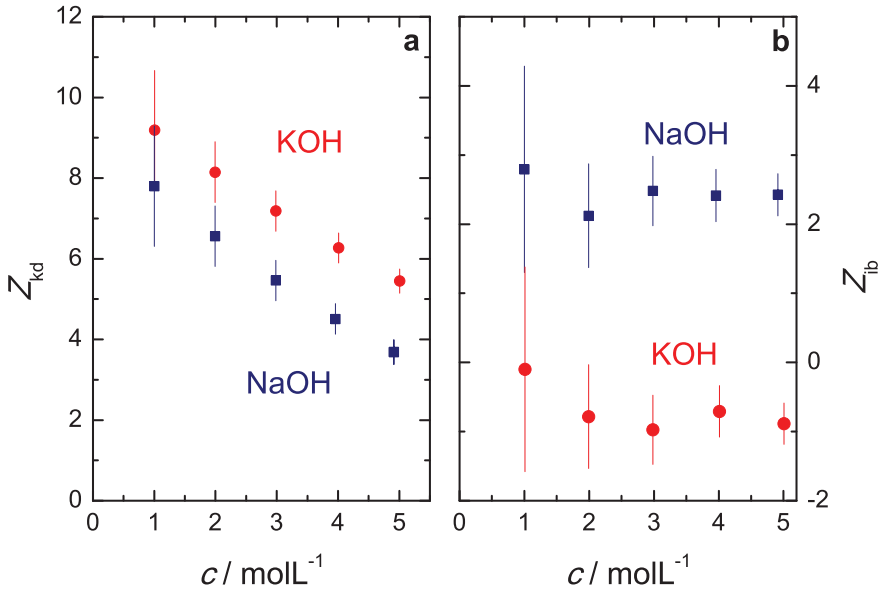

FIG. 8: (**a**) The number of water molecules Z_{kd} involved in the transport of the Na^+/K^+ and OH^- and ions. (**b**) The effective hydration number, Z_{ib} as a function of the concentration NaOH (■) and KOH (●).

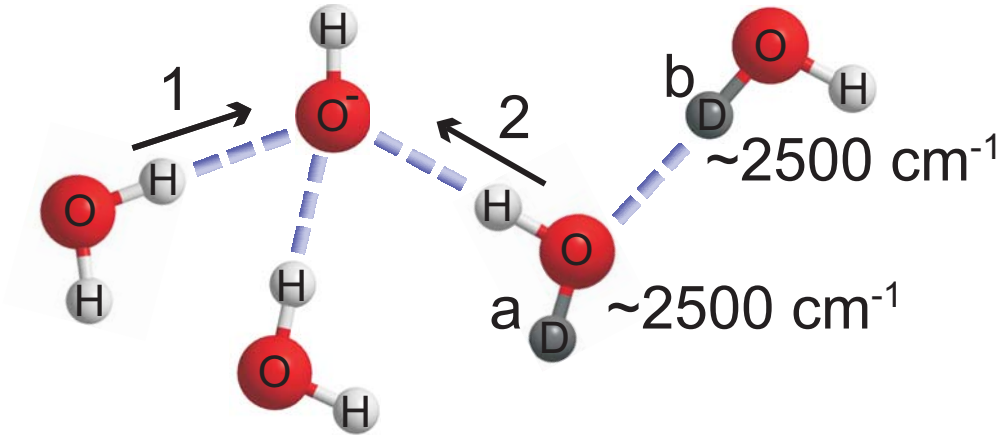

FIG. 9: Schematic presentation of proton transfer events (1,2) that affect the vibrational relaxation of excited O–D oscillators with a frequency of ∼2500 cm^{-1} located in the first (a) or second (b) hydration shell of OH^-.